Astronomy & Astrophysics manuscript no. AA6825
February 12, 2007

Whiting 1:the youngest globular cluster associated with the Sgr dSph⋆,⋆⋆

Giovanni Carraro[1], Robert Zinn[2], and Christian Moni Bidin[3]

[1] Dipartimento di Astronomia, Università di Padova, Vicolo Osservatorio 2, I-35122 Padova, Italy
e-mail: giovanni.carraro@unipd.it
[2] Astronomy Department, Yale University, P.O. Box 208101, New Haven, CT 06511, USA
e-mail: robert.zinn@yale.edu
[3] Departamento de Astronomía, Universidad de Chile, Casilla 36-D, Santiago, Chile
e-mail: mbidin@das.uchile.cl

Received .....; accepted....

ABSTRACT

Context. Recently, Carraro (2005) drew attention to the remarkable star cluster Whiting 1 by showing that it lies about 40 kpc from the Sun and is therefore unquestionably a member of the Galactic halo (b=-60.6 deg.). Its Color Magnitude Diagram (CMD) indicated that Whiting 1 is very young (~5 Gyrs) for a globular cluster. It is very likely that Whiting 1 originated in a dwarf galaxy that has since been disrupted by the Milky Way.
Aims. The main goals of this investigation were to constrain better the age, metallicity, and distance of Whiting 1 and to assess whether it belongs to a stellar stream from the Sagittarius Dwarf Spheroidal Galaxy (Sgr dSph).
Methods. Deep CCD photometry in the BVI pass-bands obtained with the VLT is used to improve the quality of the CMD and to determine the cluster's luminosity function and surface density profile. High-resolution spectrograms obtained with Magellan are used to measure the cluster's radial velocity and to place limits on its possible metallicity. The measurements of distance and radial velocity are used to test the cluster's membership in the stellar streams from the Sgr dSph.
Results. From our CMD of Whiting 1, we derive new estimates for the cluster's age ($6.5^{+1.0}_{-0.5}$ Gyrs), metallicity (Z=0.004±0.001, [Fe/H] = -0.65), and distance ($29.4^{+1.8}_{-2.0}$ kpc). From echelle spectrograms of three stars, we obtain -130.6±1.8 km/s for the cluster's radial velocity and show from measurements of two infra-red CaII lines that the [Fe/H] of the cluster probably lies in the range -1.1 to -0.4. Both the luminosity function and the surface density profile suggest that the cluster has undergone tidal stripping by the Milky Way. We demonstrate that the position of Whiting 1 on the sky, its distance from the Sun, and its radial velocity are identical to within the errors of both the theoretical predictions of the trailing stream of stars from the Sgr dSph galaxy and the previous observations of the M giant stars that delineate the streams.
Conclusions. With the addition of Whiting 1, there is now strong evidence that 6 globular clusters formed within the Sgr dSph. Whiting 1 is particularly interesting because it is the youngest and among the most metal rich. The relatively young age of Whiting 1 demonstrates that this dwarf galaxy was able to form star clusters for a period of at least 6 Gyr, and the age and metallicity of Whiting 1 are consistent with the age-metallicity relationship in the main body of the Sgr dSph. The presence now of Whiting 1 in the Galactic halo provides additional support for the view that the young halo clusters originated in dwarf galaxies that have been accreted by the Milky Way.

1. Introduction

The Milky Way galaxy harbors approximately 150 globular clusters (Harris 1996 and later revisions) and thousands of open clusters. Much of what we know about the evolution of the Galactic stellar populations has been gained through the measurement of the chemical compositions and the ages of these clusters. We know, for example, that the bulk of the globular clusters formed early in the evolution of the Milky Way, roughly 12 Gyrs ago (e.g., Salaris & Weiss 2002), whereas the onset of star formation in the thin disk, as indicated by the oldest open clusters, started later, after a hiatus of a few Gyrs (Carraro et al. 1999). The ages of the metal-rich globular clusters, some of which belong to the thick disk while others are part of the bulge, fall roughly in this age gap. However, there is a sizable spread in age among the globular clusters in the halo, and the youngest of them, e.g., Palomar 1 (Rosenberg et al. 1998a), Palomar 12 (Rosenberg et al. 1998b), Ruprecht 106 (Buonanno et al. 1994) and Whiting 1 (Carraro 2005), are significantly younger than the globular cluster 47 Tuc, the prototypical thick disk globular cluster. In fact, these young halo clusters overlap in age with the oldest open clusters. While the origin of these clusters is anomalous in a scenario where the halo and the disk are the first and last stages of an evolutionary sequence, they are explained naturally in the hierarchical picture of galaxy evolution whereby large galaxies are built through the accretion of many smaller ones (see Freeman & Bland-Hawthorne 2002 for a review). The dwarf galaxies that were accreted experienced their own histories of star and star cluster formation. The galaxies accreted at the earliest epochs, the most numerous ones according to models (e.g., Bullock & Johnston 2005), had a relatively short time to produce stars and

Send offprint requests to: G. Carraro

⋆ Based on observations with the ESO VLT at the Paranal Observatory, under the program 76.D-0128.

⋆⋆ This paper includes data gathered with the 6.5 meter Magellan Telescopes located at Las Campanas Observatory, Chile.

Table 1. Radial velocity of the 3 Whiting 1 stars.

ID	α(2000.0)	δ(2000.0)	B	V	I	$\frac{S}{N}$	RV
	hh:mm:sec	$o{:}r{:}''$					[km/sec]
6	02:02:57.1	-03:15:07.7	19.28	18.00	16.51	30	-131.1±2.8
7	02:02:52.7	-03:15:56.2	19.07	18.15	17.16	30	-130.5±3.5
8	02:02:55.2	-03:14:48.7	19.06	18.14	17.15	30	-130.1±3.1

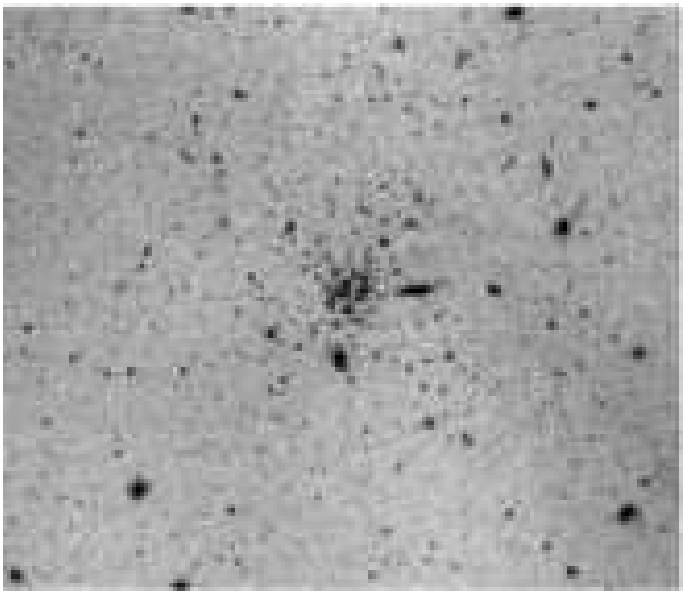

Fig. 1. A 1200 secs B image of the Whiting 1 field. North is up, East to the left, and the image is 6.8 arcmin on a side.

clusters, whereas the ones accreted most recently had a larger span of time available. It is therefore attractive, as many other authors have, to identify the young globular clusters as relatively recent additions to the Galactic halo that had their origins in disrupted dwarf galaxies (e.g., Searle and Zinn 1978). The most clear-cut example of this is the current tidal destruction of the Sagittarius Dwarf Spheroidal (Sgr dSph) galaxy, which is probably the origin of Pal 12 (Dinescu et al. 2000; Martinez-Delgado et al 2002; Cohen 2004) and Whiting 1 (see below). The recent detections of other stellar streams and substructures in the halo, which appear to be unrelated to the Sgr dSph (Newberg et al. 2002, Duffau et al. 2006, Belokurov et al. 2006, Grillmair and Dionatos 2006; Grillmair 2006), is powerful evidence that the destruction of Sgr is not an isolated event in an otherwise orderly evolution from halo to disk, but merely the most recent episode of halo building through the accretion of satellite galaxies.

The youngest of the Galactic globular clusters, Whiting 1, was discovered recently by Whiting et al. (2002), who suspected it was a young open cluster. More recently, Carraro (2005) demonstrated that this cluster cannot be in the Galactic disk, but must be in the halo. From shallow photometry (V ~ 22-23) obtained with the Yale 1.0m telescope at CTIO, he derived an age of roughly 5 Gyr, a metallicity of Z=0.004 ([Fe/H]= -0.7), and a distance of ~ 40 kpc from the Sun. Since these are exceptional properties for an outer halo cluster, we have obtained deeper photometry to constrain better these parameters. We have also measured its radial velocity so that its membership in the trailing stream of stars from the Sgr dSph galaxy, which lies along the same line of sight, can be examined.

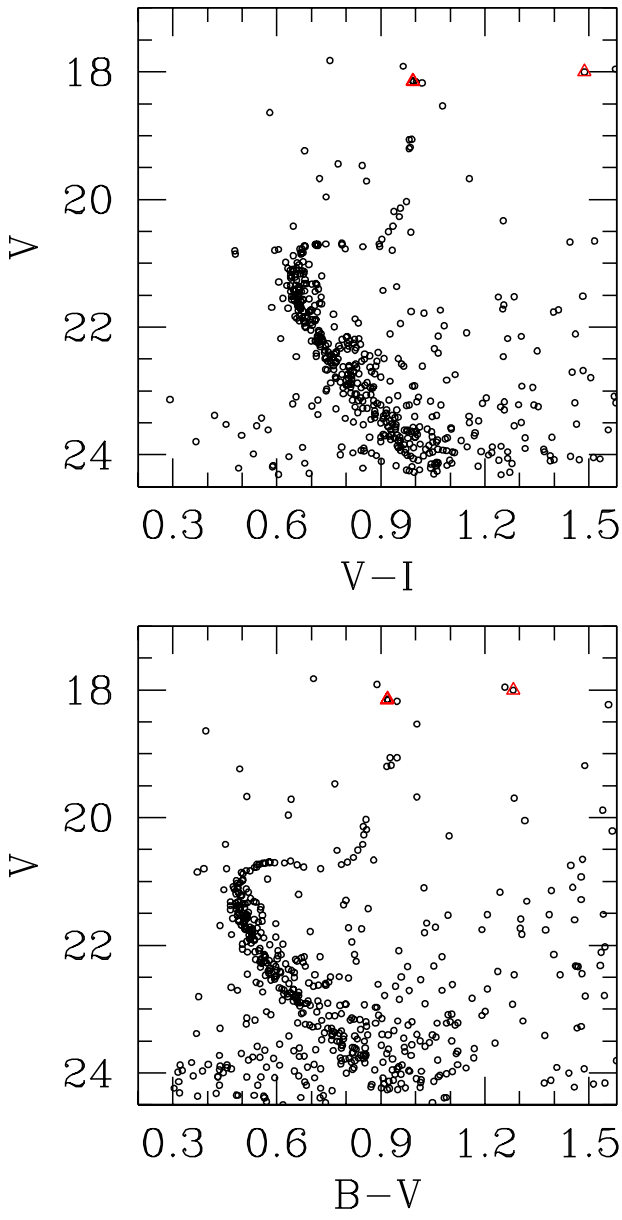

Fig. 2. CMDs in the V vs B-V (lower panel) and V vs (V-I) (upper panel) planes of the stars within a radius of 1 arcmin and having photometric errors lower than 0.06 in B, V and I. Open triangles indicate the 3 stars observed spectroscopically.

2. Observations and Data Reduction

2.1. Photometry

On the nights of 10 and 11 October 2005, Whiting 1 was observed in the BVI filter bands with the Very Large Telescope UT2 Kueyen and the FORS1 CCD camera. Six deep exposures were taken (2x1200 sec in B, 2x700 sec in each V and I) on those nights, which had photometric conditions and an average seeing of 0.8 arcsec. The camera has a scale of 0.2 arcsec per pixel and an array of 2048x2048 pixels. An example of one of the 6.8x6.8 arcmin images of Whiting 1 is shown in Fig. 1. The standard

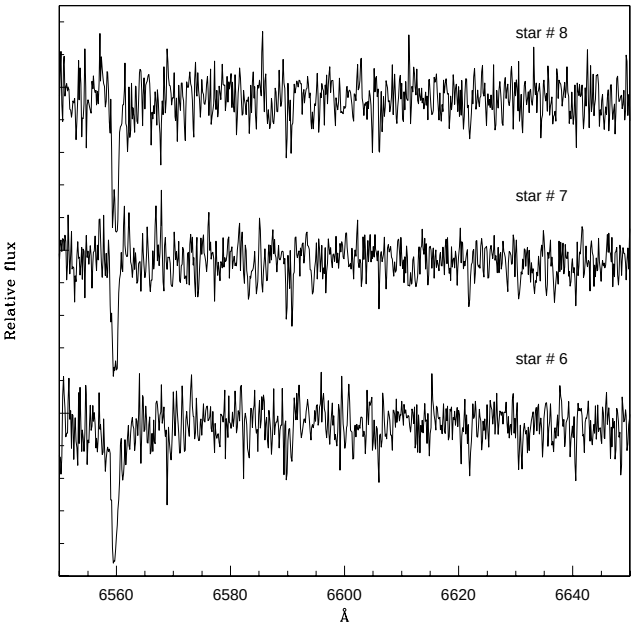

Fig. 3. MIKE spectra of the 3 Whiting 1 stars (see also Table 1 and Fig. 2).

IRAF [1] routines were used to reduce the raw images. Using the psf-fitting routines of DAOPHOT and ALLSTAR (Stetson 1994) in the IRAF environment, we measured instrumental magnitudes for all of the stars in the field. These magnitudes were transformed to the standard system using as standards the shallower, calibrated photometry of Carraro (2005).

2.2. Color Magnitude Diagrams

Carraro (2005) estimated that Whiting 1 has a radius of approximately 1 arcmin. The stars that we measured within that radius and having photometric errors less than 0.06 mag are plotted in the CMDs in Fig. 2. These diagrams are a substantial improvement over the ones measured by Carraro (2005) in that they go roughly 4 mag. deeper and define more precisely the principal sequences of the CMD. The turn off (TO) from the main-sequence is quite clear and is located at V=21.2, (B-V)=0.48, and (V-I) = 0.63). There appears to be a sequence running roughly parallel to the main-sequence that may be composed of binary stars. Although the red giant branch (RGB) is sparsely populated, its lower part is well traced. A clump of stars is located at V = 18.3, (B-V)=0.95, and (V-I) = 0.98, which is consistent with the core helium burning phase of evolution.

2.3. Spectroscopy

Echelle spectrograms of stars #6, #7, and #8 (see Table 1 and Fig. 3) were obtained with integrations of 1200s per star on 2006 September 26 with the Magellan Inamori Kyocera Echelle (MIKE) spectrograph mounted on the Nasmyth focus of Landon Clay 6.5m telescope at the Magellan Observatory. Data were obtained with both the blue and red arms, but only the red spectra (4950-9500 Å) had sufficient signal to noise ($\frac{S}{N}$) to be useful. The spectra in part of this range are shown in Fig.3. The slit was 1 arcsec wide, which yielded a resolution R=22000, and the CCD was binned in steps of 3 pixels in the dispersion direction. The excellent seeing may have caused a higher resolution and a slight under sampling because of the binning. We used quartz lamp images with the diffuser in position for flat field correction, and the wavelength calibration was performed with ThAr lamp images that were taken just before and after three stellar exposures. The dark current was checked by examining several dark exposures and was found to be insignificant. The optimum algorithm (Horne 1986) was used to extract the spectra, which were also sky-subtracted and normalized using IRAF routines.

Radial velocity (RV) measurements were performed with the cross-correlation (CC) technique (Tonry & Davis 1979) in the spectral range 5000-6700 Å, which avoided the strong telluric bands at longer wavelengths. We also made some measurements at other wavelengths and obtained results that were always consistent to within the errors. For a template, we used a synthetic spectrum of a K3III star, but also checked the results with other spectra from the library of Coehlo et al. (2005) that differed in atmospheric parameters and metallicity. The height of the peak of the CC function decreased when there were relatively large differences between the template and target spectra, but the radial velocities remained stable. The results of the CCs were corrected for: 1) heliocentric correction, 2) systematic offsets in the wavelength calibrations, which were estimated from measurements of the strong telluric bands in twilight sky exposures, and shifts due to star centering in the slit, 3) a systematic offset (≈1.0 km/s) from RV standard stars and from twilight sky exposures, which may result from the use of synthetic spectra in the CCs. The errors quoted in Table 1 were calculated from the quadratic sum of all sources of error: CC measurements, wavelength calibrations, and the corrections stated above. The RVs of the three stars are very similar to each other. Under the reasonable assumption that all three are cluster members, we obtain from their mean value a velocity of -130.6±1.8 km/s for the cluster.

3. Fundamental parameters

3.1. Estimates of reddening, age, metallicity, and distance modulus from the CMD

By fitting isochrones for different ages and metallicity to the CMD of Whiting 1, we can place limits on its reddening and distance modulus. In Fig. 4, the CMD of Whiting 1 is compared with theoretical isochrones that have been calculated by the Padova group (Girardi et al. 20002) for Y=0.24 and solar mixes of elements. The metallicity was fixed, and then the age, distance modulus, and reddening were adjusted until a match to the main-sequence, subgiant branch, and lower RGB was obtained. However, one of these fits produces an unphysical value for the reddening, and another produces a very unlikely value. The fit shown in the left panel is for a relatively high metallicity (Z=0.008, [Fe/H] = -0.37). In order to match the relatively blue colors observed for the Whiting 1 stars, it was necessary to assume the cluster suffers from a *negative* reddening. The result obtained with a much lower metallicity (Z=0.001, [Fe/H] = -1.30) is shown in the right panel of Fig. 4. In this case, the Whiting 1 stars are redder than the isochrones by a considerable amount, and to make them match up, it was necessary to assume a reddening of E(B-V) = 0.18. This value is untenably larger than the value (0.03) that the dust maps of Schlegel et al. (1998)

[1] IRAF is distributed by the National Optical Astronomy Observatories, which are operated by the Association of Universities for Research in Astronomy, Inc., under cooperative agreement with the National Science Foundation.

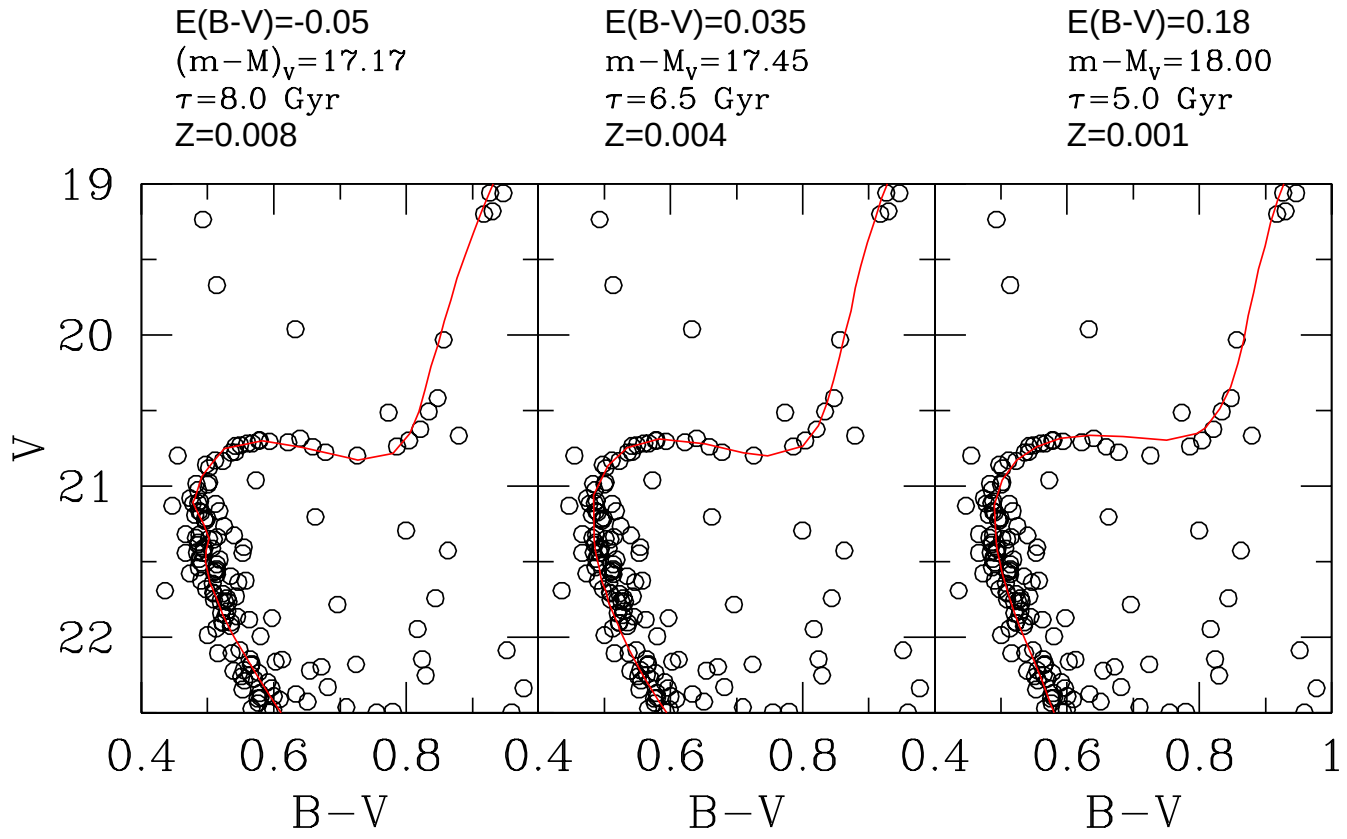

Fig. 4. Isochrone solutions for Whiting 1: three different age-metallicity combinations are explored, and each isochrone has been shifted by the reddening and apparent distance modulus indicated.

indicate is the average reddening in a 6 sq. arcmin area around the cluster. At the Galactic latitude of Whiting 1 (-60.64) only a small variation in reddening is expected over this area. The results obtained with these two metallicities suggest that an intermediate value may produce reasonable results. The middle panel shows the results obtained with the metallicity Z=0.004 ([Fe/H] = -0.65), which produces a better match to CMD than either of the other two and also a reddening value that is consistent with the maps of Schlegel et al. (1998).

By fine tuning of the fit in the middle panel, we estimate that the age and metallicity of Whiting 1 is $6.5^{+1.0}_{-0.5}$ Gyr. and Z=0.004±0.001, respectively. By shifting the isochrone in the middle panel within acceptable limits, we estimate that the errors in E(B-V) and (m-M)$_V$ are 0.01 and 0.1, respectively. These values and an assumed ratio of total to selective (R=$\frac{A_V}{E(B-V)}$) of 3.1 yield $29.4^{+1.8}_{-2.0}$ kpc for the heliocentric distance of Whiting 1. If we place the Sun at 8.0 kpc from the Galactic Center, Whiting 1 (l=161.62, b=-60.64) has a mean Galactocentric distance of 33.9 kpc. Its Cartesian coordinates (Harris 1996) are X=-21.7, Y=4.5, and Z=-25.6 kpc.

3.2. Estimate of metallicity from the infrared CaII lines

The $\frac{S}{N}$ of the spectrograms are too low for a determination of metal abundance of Whiting 1 by the standard technique of comparing the equivalent widths of weak metal lines with synthetic spectra calculations. We can, however, determine a rough estimate from the pseudo-equivalent widths of the strong CaII lines in the near infrared, which were included in one of the orders of the echelle spectrograms. Several studies have shown that measurements of these lines in low-dispersion spectrograms of red giants provide precise rankings of globular clusters by [Fe/H], and the recent studies by Pont et al. (2004), Cole et al. (2004), and Carrera et al. (2007) have shown that this method can be applied without modification to red giants in open clusters that have ages greater than about 3 Gyr.

Only one (#6) of the three stars observed in Whiting 1 lies near the RGB. The other two appear to be part of a red clump of core helium burning stars. Red clump stars (or red horizontal branch stars in globular clusters) have been seldom included in studies of the CaII lines, which have concentrated on stars on the RGB. However, a few of these stars in the open cluster M 67 and the globular cluster M 71 were included in the catalogue of CaII line strengths measured by Cenarro et al. (2001). According to Sandquist (2004) and references therein, M 67 is 4 Gyrs old and has approximately solar composition. M71 is much older, ∼10 Gyrs, and more metal poor, [Fe/H] ∼-0.7 (e.g., Salaris & Weiss 2002). In the upper diagram of Fig. 5, we have plotted the index CaT measured by Cenarro et al. (2001) against M$_V$, using the distance moduli listed by Sandquist (2004) and by Harris (1996). This diagram shows that the red clump stars (or red HB stars) in M 67 and M 71 do not deviate systematically from the sequence of RGB stars. While the RGB stars are cooler than the red clump stars of the same M$_V$, which weakens CaT in this effective temperature range, they also have lower gravities, which

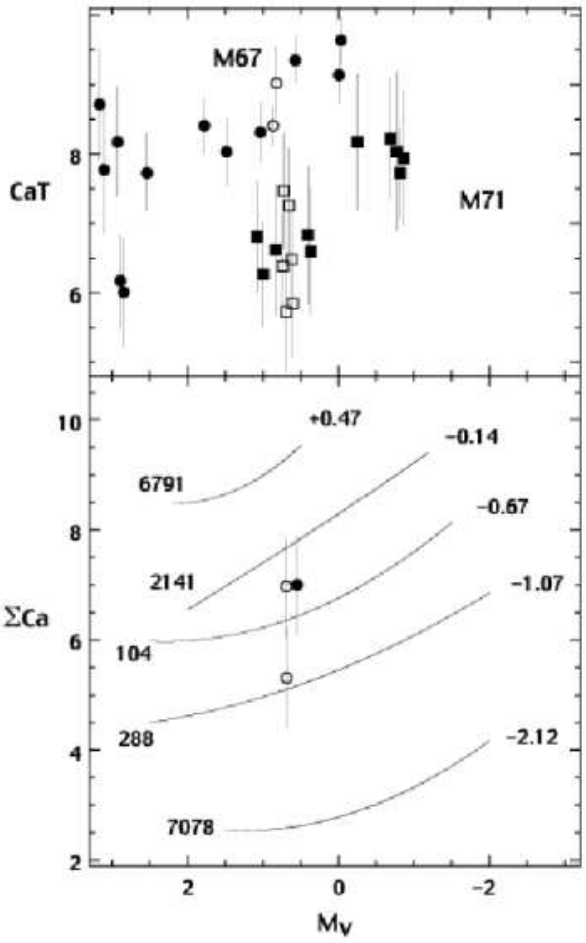

Fig. 5. In the upper diagram, the CaT indices of Cenarro et al. (2001) for red giants and red clump stars (solid and open symbols, respectively) in M67 and M71 are plotted against Mv. In the lower diagram, the ΣCa indices for the red giant and the red clump stars (solid and open circles) in Whiting 1 are compared with the cluster sequences observed by Carrera et al. (2007). The [Fe/H] values that label the cluster sequences are on the metallicity scale of Carretta & Gratton (1997).

strengthens CaT (see Cenarro et al. 2002). The upper diagram in Fig. 5 suggests that the temperature and surface gravities differences offset each other to the precisions of the measurements. There is therefore some justification for treating all three stars in Whiting 1 as if they belong to the RGB of the cluster.

One order of the spectrograms of the Whiting 1 stars cover the range 8470-8710 Å, and over this range the $\frac{S}{N}$ varies between ∼7 and ∼10. While this low $\frac{S}{N}$ would preclude measurement of the CaII line strengths in the low-resolution spectrograms (R ∼ 2000) normally employed to measure them, they are measurable in our much higher resolution spectrograms. The wavelength ranges used by Cenarro et al. (2001) to define the CaT index extend both bluer and redder than the Whiting 1 spectrograms. The ranges used by Armandroff & Da Costa (1991, hereafter AD) to measure the two strongest of the CaII lines extend insignificant amounts beyond the limits of our spectrograms, and it is possible to measure their Ca II index. However, AD did not observe any stars as low in luminosity as the Whiting 1 ones. Even lower luminosity ones have been measured recently by Carrera et al (2007). Although the CaII index (ΣCa) defined by Carrera et al., which is based on the same side bands as the CaT index, is not measurable in our spectrograms, they have shown that there is a tight correlation between the AD index and ΣCa. We have therefore followed closely the measuring technique of AD, which consists of fitting a straight line to the intensities in wavelength bands on either side of the two strongest (λ8542 & λ8662) of the three CaII lines. The straight lines set the pseudo-continua for the line profiles, which following AD were fit by Gaussian profiles. To explore the effects of low $\frac{S}{N}$ on the measurements, we smoothed the spectrograms by varying amounts to mimic ones of higher $\frac{S}{N}$ but lower resolution and found no significant systematic offsets in the AD index. This is consistent with the results that Carrera et al. (2007) found when comparing spectrograms of the same stars taken with different spectrographs and resolutions. We also fit the Gaussian profiles to the Whiting 1 stars after varying the height of the pseudo-continua within reasonable limits to get an estimate of the uncertainties in our measurements. Finally, we used the transformation equation given by Carrera et al. (2007) to transform our measurements into values of ΣCa.

In the lower panel of Figure 5, we compare the ΣCa indices of the Whiting 1 stars with the sequences observed by Carrera et al. (2007) in 3 globular clusters (NGC 104, 288, 7078) and two open clusters (NGC 6791, 2141). A distance modulus of $(m\text{-}M)_V$ = 17.45 (see above) was adopted for Whiting 1. All reasonable ones yield similar values of [Fe/H]. As expected from the upper diagram, there is no significant offset, to within the errors, between the two red clump stars and the one RGB star in Whiting 1, and the mean position of the 3 stars suggests a metallicity near [Fe/H] = -0.7. The calibrations (Carrera et al. 2007) of ΣCa in terms of [Fe/H] on the metallicity scales of Carretta & Gratton (1997), Kraft & Ivans (2003), and Zinn & West (1984) yields mean values of -0.65±0.20, -0.82±0.20, and -0.83±0.26, respectively. These errors include our estimates of the random errors in our measurements and the transformation of the AD indices to ΣCa. We caution that they may be too small because we do not have any repeated observations or observations in common with other observers that would enable us to measure better our random errors and correct for any systematic ones. Nonetheless, these measurements indicate that the [Fe/H] of Whiting 1 probably lies within the range of -0.4 to -1.1, which is consistent with what we found above from comparing isochrones to the CMD.

Table 2. Completeness results for three different zones in Whiting 1.

V	$R \leq 0'.75$	$0'.75 \leq R \leq 1'.50$	$1'.50 \leq R \leq 2'.25$
21.0	95.2	99.9	99.9
21.5	96.9	99.9	99.8
22.0	93.6	98.6	98.2
22.5	95.0	97.5	97.1
23.0	88.5	88.1	96.5
23.5	79.6	82.1	92.4
24.0	62.5	70.9	89.1

3.3. The Luminosity Function

With the goal of measuring the integrated apparent magnitude of Whiting 1 (V_t) and hence its absolute magnitude, we have determined its luminosity function (LF) in different radial zones. To do this, we estimated the completeness of our photometry by running experiments with artificial stars. First, we divided

the cluster into 3 concentric rings centered on the cluster: r ≤ 0.75, 0.75 ≤ r ≤ 1.50, and 1.50 ≤ r ≤ 2.25. Within these rings, we counted 204, 127, and 107 stars brighter than V =24. We then used the routine ADDSTAR within DAOPHOT to insert 1000 artificial stars at random positions over the whole field and within the magnitude range of the real stars. This number of artificial stars was chosen so that a reasonable number of them (about 30% of the real star population) would lie within the cluster radius (∼1.5 arcmin.). This was done for both the long and the short exposures. We then reduced the images with the artificial stars in exactly the same manner as the real images. The ratio of the number of artificial stars recovered by ALLSTAR to the number inserted defines the completeness. This experiment was run 10 times using a different seed number with the random number generator that ADDSTAR uses in the calculation of the positions and magnitudes of the artificial stars. The mean values that were found for the completeness in the three radial zones are listed in Table 2.

To construct the faint part of the LF, we placed two curves on either side of the subgiant branch and the main-sequence and parallel to the ridge line defined by the concentration of cluster stars. We then counted the number stars within this band that have 21.0 ≤ V ≤ 24.0. In exactly the same way, we counted the stars in the field, far beyond the cluster radius, that lie in the same region of the CMD. This field contribution was normalized to the areas of the radial zones and subtracted from each of the magnitude bins of the LF. The background and completeness corrected LF for the three radial zones is shown in Fig. 5, where the error bars are the ones indicated by Poisson statistics. In the innermost and outermost regions and nearly so in the intermediate region, the LF flattens out toward faint magnitudes. In *normal* globular clusters the LF continues to rise. Flat LFs that resemble Whiting 1's have been observed in globular clusters that appear to be undergoing tidal stripping by the gravitational field of the Milky Way (e.g., Pal 5, Koch et al. 2004; Pal 13, Cote et al. 2002).

To obtain V_t, we combined the three LFs in Fig. 5 and added the brighter stars that lie either close to expected location of the RGB or are part of the red clump. Integration of this combined LF yields Vt = 15.03. This value and the distance modulus of $(m\text{-}M)_V$ = 17.45 yield M_V = -2.42 for Whiting 1. The uncertainty in this value is ±0.1 and possibly larger, for we cannot be certain that all of the bright stars have been included or that the field stars have been removed. Despite this uncertainty, it is clear that Whiting 1 is among the least luminous globular clusters known. Among the ∼150 Galactic globular clusters, only 4 (Pal 1, E3, AM4, Willman 1, Segue 1) in addition to Whiting 1 have M_V larger than -3 (Harris 1996, 2003 ed.; Willman et al. 2006; Belokourov et al. 2006).

3.4. The surface density profile

If, as suggested by its LF, Whiting 1 has experienced tidal stripping, its surface density profile is expected to be also abnormal. This profile was constructed by counting the stars in our catalogue of V photometry that lie within the color range 0.6 ≤ $V - I$ ≤ 1.4 and are brighter than V=24.0. The paucity of cluster stars (see Fig. 1) made uncertain the location of the cluster center, and we defined it by the peaks in the histograms of the number of star images per distance interval in the X (RA) and Y (DEC) directions. To measure the background of field stars, we subtracted from the catalogue the stars lying less than 1.5 arcmin from the cluster center (a preliminary radius) and then counted the remaining stars that fell within the same magnitude and color ranges that were used when counting the cluster stars.

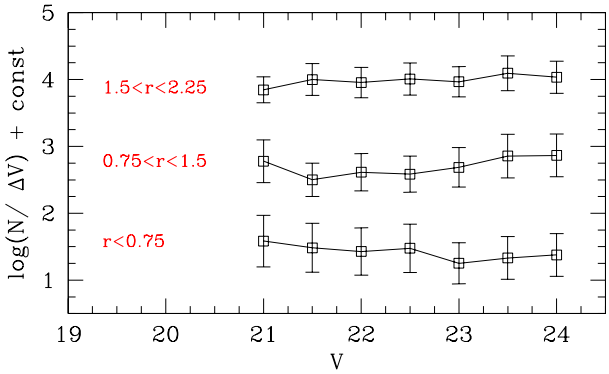

Fig. 6. Completeness and background corrected LF of Whiting 1 for the three indicated rings. For clarity, the LF's for the outer and intermediate rings have been shifted upward by 3.0 and 1.5, respectively.

This yielded 3.35 stars per square arcmin for the background, which is indicated in Fig. 7 by the symbol Σ_B. Contributing to this background are stars belonging to the trailing stream of stars from the Sgr dSph galaxy, in which Whiting 1 is immersed (see below).

Unlike the surface density profiles of many globular clusters, the profile of Whiting 1 (Fig. 7) cannot be approximated with a single King profile. If a King profile is fit to the outer part (log R ≥ 1.8 arcsec), it grossly underestimates the density in the inner part, which is more secure statistically. We show in Fig. 7 the opposite case where a King profile is fit to the innermost 4 points, which produces a very poor fit to the outermost points. Compared to this profile there is an excess of stars that follow a power law ($R^{-\gamma}$) density profile with $\gamma \approx 1.8$. Other globular clusters that are suspected to have undergone tidal stripping (see Grillmair et al. 1995; Cote et al. 2002) have profiles that are similar to the one of Whiting 1. Their inner parts are well represented by a King profile, but beyond the tidal radius of the profile there are *extra-tidal* stars that follow a power law slope. Since this behavior is also expected theoretically (e.g., Johnston et al. 1999), we conclude that the surface density profile of Whiting 1, as well as its LF, suggests that it is losing mass by tidal stripping.

4. Membership in the Sagittarius Trailing Stream

As discussed by Carraro (2005) and above, Whiting 1 is several Gyrs younger than any other star cluster in the Galactic halo. While the presence of such a young object in the halo would have once seemed mysterious, this is no longer so because the halo is now known to be crisscrossed with stellar streams from disrupted satellite galaxies (see above). We show below that the position and radial velocity of Whiting 1 are consistent with membership in the stream of stars trailing behind the Sgr dSph galaxy as it orbits the Milky Way.

In order to compare Whiting 1 with models of the Sgr streams and with stars that constitute the streams, we have computed its longitude ($\lambda_\odot$) and latitude ($\beta_\odot$) in the Sgr orbital plane as viewed from the Sun, and its radial velocity (Vgsr) in the Galactic rest frame ($\lambda_\odot$ =102^o.91, $\beta_\odot$=+1^o.33, Vgsr = -105.0 km sec-1). In these calculations, we have followed the procedures and the choice of solar motion used by Majewski et al. (2003,

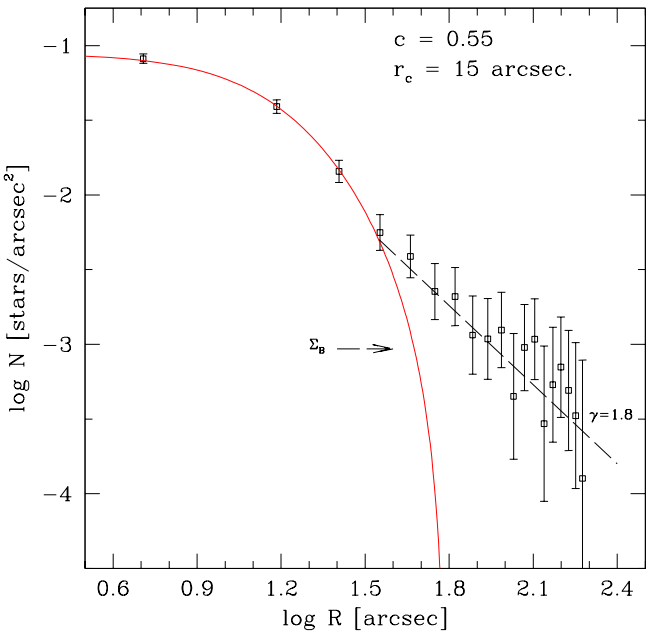

Fig. 7. Radial surface density profile of Whiting 1. The solid line is a King profile, while the dashed line is a power-law profile for the extra-tidal stars. The density of the background is indicated by Σ_B. See text for more details.

2004)[2] so that the results for Whiting 1 could be directly compared with theirs for M giants and with the theoretical models of Law et al. (2005). In the Sgr coordinate system, the main body of Sgr is located at $\lambda_\odot = 0^o$, and the $\lambda_\odot$ increases in the direction of the trailing stream. The coordinates for Whiting 1 show that on the sky it lies in the direction to the trailing stream and very close to the orbital plane.

In upper panel of Fig. 8 is a plot of distance from the Sun (d) against $\lambda_\odot$ in which we have plotted Whiting 1, M giants with measured radial velocities (Majewski et al. 2004), and the model that Law et al. (2005) calculated under the assumption that the gravitational potential of the Milky Way is spherical in shape. The lower panel compares the values of Vgsr for these objects with the same models. Law et al. (2005) have also calculated models assuming prolate and oblate potentials. Over the ranges of $\lambda_\odot$ and d that are relevant to Whiting 1 these models produce similar distributions in the diagrams plotted in Fig. 8 (see figs. 2 and 10 in Law et al. 2005). The models of Law et al (2005) are based in part on distribution of the M giants, but over much larger regions of the sky than are included in Fig. 8. Therefore, the less than perfect match of the model to the M giants in this restricted region is not surprising. This disagreement could also be due to an underestimate of the distances to these stars (see Chou et al. 2006).

The data plotted in Fig. 8 indicate that not only does Whiting 1 lie in the direction to the Sgr trailing stream, but its distance places it within the stream of M giants and its radial velocity suggests that it and the M giants are moving on similar orbits. These data for Whiting 1 agree almost perfectly with the predictions of the models constructed by Law et al. (2005) for the Sgr streams (see Fig. 8), and are also consistent with the models calculated by Martinez-Delgado et al. (2004a) and by Helmi (2004a,b). On the basis of the above evidence, we believe that it is highly probable that Whiting 1 originated in Sgr, and in the following section, we compare its properties with the other Sgr clusters.

[2] See also http://www.astro.virgina.edu~srm4n/Sgr

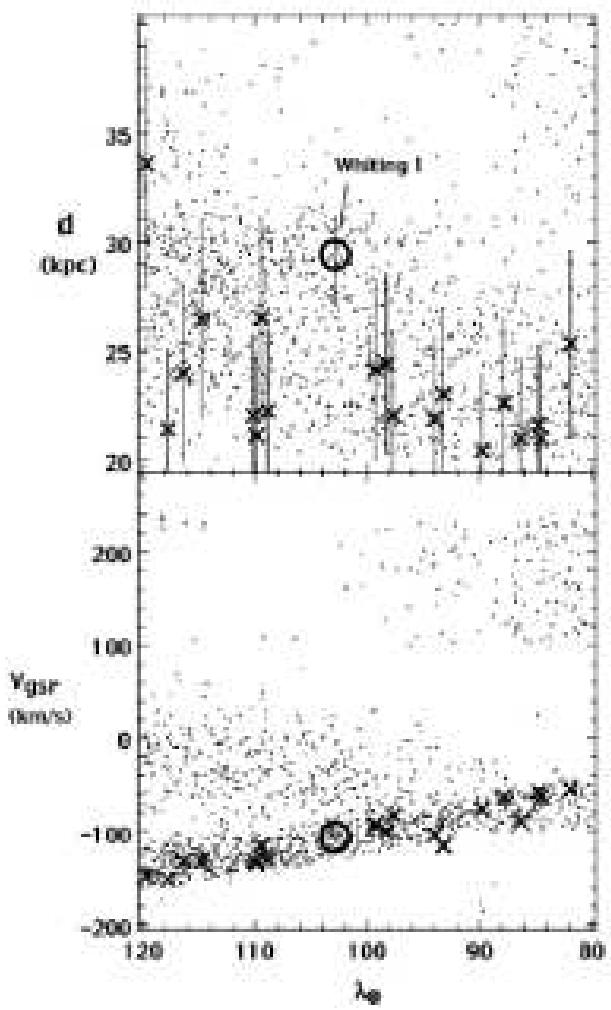

Fig. 8. Whiting 1 (open circle) and M giants (X's) from Majewski et al. (2003,2004) are compared with the model of the Sgr stream (small points) that was computed by Law et al. (2005) under the assumption that the Galactic potential is spherical. For clarity, only objects between 20 and 40 kpc from the Sun have been plotted in the two diagrams. Distance from the Sun (d) and velocity in the Galactic rest frame (Vgsr), are plotted against longitude in the Sgr orbital plane ($\lambda_\odot$ in deg.). The error bars of the velocity measurements have not been plotted because they are smaller than the symbols.

5. Whiting 1 and the star cluster family of the Sgr dSph

The main body of the Sgr dSph contains 4 globular clusters: M54, Terzan 7 and 8, and Arp 2. M54, which lies at the center of the main body, is very luminous and has an age similar to the ages of the oldest globular clusters in the Galactic halo. It is unusual for a globular cluster in having an internal metallicity spread, and several authors (e.g., Layden and Sarajedini 2000) have suggested that M54 is actually the nucleus of the galaxy,

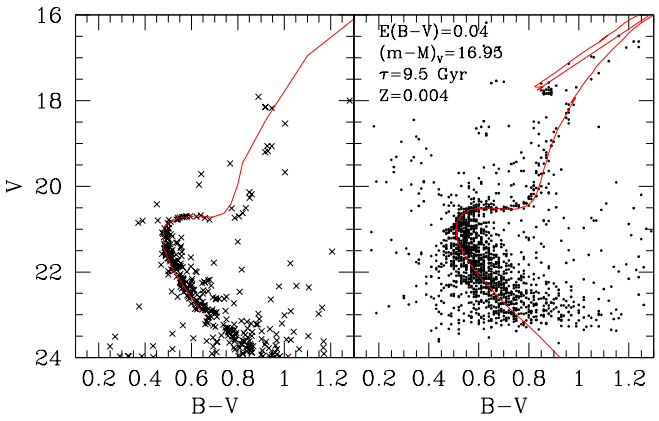

Fig. 9. Left panel: Whiting 1 stars with the fiducial sequence (solid line) of Terzan 7 (Buonanno et al. 1995) superimposed.; **Right panel**: Terzan 7 stars with a Z=0.004 isochrone (solid line) for the age of 9.5 Gyr superimposed. The isochrone has been shifted by the values of E(B-V) and (m-M)$_V$ indicated

which if correct would make Sgr a nucleated dwarf elliptical galaxy. Two of the other star clusters, Ter 8 and Arp 2, are metal-poor and old globular clusters, whereas Ter 7 is both metal-rich and young for a globular cluster (Buonanno et al. 1995).

Several authors have examined the sample of Galactic globular clusters for ones that may have originated in the Sgr dSph galaxy, with in some cases conflicting conclusions (e.g., Palma et al. 2002, Bellazzini et al. 2003; Martinez-Delgado et al. 2004b). The young and metal-rich Galactic globular cluster Palomar 12 appears to be the most likely case of a detached Sgr cluster, although some others cannot be ruled out with certainty. Dinescu et al. (2000) have shown that the orbit of Pal 12 is consistent with it once being a member of Sgr. The photometry by Martinez-Delgado et al. (2002) indicates that Pal 12 is embedded in a rich population of extra-cluster stars at the same distance from the Sun as the cluster, which is a sign that the cluster is part of stellar stream. The high-dispersion spectroscopy of red giants in Pal 12 by Cohen (2004) indicates that it has a chemical composition that is unusual for a Galactic globular cluster, but perfectly compatible with an origin in the Sgr dSph galaxy

Since Ter 7 and Pal 12 are the youngest and most metal rich of the Sgr family of star clusters, including the other clusters suspected to be members, they are the ones that are most interesting to compare with Whiting 1. While there has been no disagreement that both Ter 7 and Pal 12 are young and metal rich, the ages and metallicities that have been quoted for these clusters in the literature do vary considerably. Their unusual chemical compositions may explain why the application of the methods that are used to rank the metallicities of Galactic globular clusters from the properties of the red giant branch and from low dispersion spectroscopy have yielded conflicting results. The high dispersion spectroscopy of red giants in Ter 7 by Sbordone et al. (2005) and by Tautvaisiene et al. (2004) have yielded [Fe/H] = -0.6. Spectroscopy of red giants in Pal 12 by Cohen (2004) indicate that it has [Fe/H] = -0.8. According to these groups, both clusters have approximately solar α/Fe, which is consistent with field stars in the main body of Sgr that have similar [Fe/H] (Bonifacio et al. 2004; McWilliam and Smecker-Hane 2005; Monaco et al. 2005). Since we have estimated above that Whiting 1 has essentially the same metallicity as Ter 7, which is not far from that of Pal 12, it is relatively straightforward to compare the ages of these three clusters by simply overlaying of their CMD's. We have done this first for Pal 12 and Ter 7 by selecting the CMD's of Stetson et al. (1989) and Buonanno et al. (1995), respectively. By shifting the ridge-lines for Pal 12 by +0.07 in (B-V) and +0.6 in V, the TO regions and the horizontal branches (HB's) of Pal 12 and Ter 7 are brought into coincidence. With these shifts, there are only very small differences in magnitude and color between the ridge-lines of Pal 12 and Ter 7. The lower red giant branch of Ter 7 may lie slightly to the red of Pal 12's, which is consistent with Ter 7 being more metal-rich by a small amount, as suggested by the spectroscopic studies. However, this could also be nothing more than observational error. The overall excellent match of ridge-lines indicates that Ter 7 and Pal 12 are essentially coeval (Δt less than 1 Gyr).

The CMD of Whiting 1 is compared with the ridge-line of Ter 7 (Buonanno et al. 1995) in the left panel of Fig. 9. Because the HB of Whiting 1 is defined by very few stars and resembles more a red clump than the HB of a globular cluster, we have not used it in this comparison. Instead, the ridge-line of Ter 7 was shifted by -0.04 in B-V and +0.2 in V in order to bring the TO regions of the two clusters into coincidence. Fig. 9 shows that after registration of the TO regions, there is a large difference between the red giant branches of Whiting 1 and Ter 7 in the sense expected if Whiting 1 is the younger cluster. How much younger is estimated in the right-hand panel of Fig. 9, where an isochrone from the same set that was used to date Whiting 1is compared with the photometry of Ter 7 by Buonanno et al. (1995). By fine-tuning the fit, we estimate the age of Ter 7 is $9.5^{+0.5}_{-1.0}$ Gyrs., which suggests that Whiting 1 is approximately 3 Gyrs. younger than Ter 7 and Pal 12, which as noted above are near clones.

The metal-poor clusters in Sgr appear to be approximately coeval with the oldest Galactic globular clusters (e.g., Layden and Sarajedini 2000), which according to recent studies (e.g., Salaris and Weiss 2002) have ages of 12 to 13 Gyrs. The identification of Whiting 1 with Sgr suggests that this galaxy was able to form star clusters for $\approx$ 6 Gyrs. The ages and metallicities of Ter 7 and Pal 12 indicate that [Fe/H] rose relatively rapidly in over the first few Gyrs to $\approx$ -0.6. It appears to have been essentially level from the formation of those clusters until at least the formation of Whiting 1 $\approx$ 3 Gyrs. later. This is consistent with the recent conclusion of Bellazzini et al. (2006) that the stellar population in the core of Sgr has [Fe/H] $\approx$ -0.6 and age $\approx$ 8 Gyrs. Observations of the red giants clearly indicate that [Fe/H] eventually rose to a higher value ($\approx$ 0) than found in any of the known Sgr clusters (e.g., Bonifacio et al. 2004; McWilliam and Smecker-Hane 2005; Monaco et al. 2005). Because there is a gradient of decreasing [Fe/H] with distance from the center of the main body, and because objects in the streams are most likely detached from the outskirts of the galaxy (see Chou et al. 2006), the use of Whiting 1 and Pal 12 to anchor the age-[Fe/H] relation must be viewed with some caution.

The on-going destruction of the Sgr dSph has so far deposited in the Galactic halo two remarkably young globular clusters, Pal 12 and Whiting 1. Its final destruction will contribute another young cluster Ter 7, the more normal ones Arp 2 and Ter 8, and M54, the suspected nucleus. It is possible that other Sgr clusters remain to be discovered in its tidal streams and that some Galactic globular clusters besides Pal 12 and Whiting 1 will be definitely identified with Sgr. The drama being played out today by the destruction of this dwarf galaxy may be characteristic of many earlier accretion events, which are speculated to have populated the Galactic halo with stars and star clusters (e.g., Bullock and Johnston 2005; Searle and Zinn 1978). Since

several other stellar streams have been already identified in the halo, the identification of star clusters with these or other streams may not be far behind.

6. Summary and Conclusions

The photometry reported here has confirmed the major conclusions of Carraro (2005) that Whiting 1 lies in the outer Galactic halo and is unusually young for a globular cluster. We derived here a somewhat larger age for the cluster (6.5 Gyrs) and a smaller distance from the Sun (29.4 kpc). The luminosity function and the surface density profile that we obtained suggest that Whiting 1 has been losing mass via tidal stripping by the Milky Way. The new distance to Whiting 1 places it within the trailing stream of stars from the Sgr dSph galaxy. The radial velocity that we have measured for the cluster is very similar to the ones of M giants in the stream and is in excellent agreement with theoretical predictions for the stream at its location. The age and metallicity derived here for Whiting 1 are consistent with the age-metallicity relationship of Sgr. We conclude that Whiting 1 is another example of a young globular cluster that has been detached from its parent dwarf galaxy and is now a member of the Galactic halo.

Acknowledgements. This research was part of a joint project between Universidad de Chile and Yale University, partially funded by the Fundacion Andes. RZ was supported by National Science Foundation grant AST-05-07364. GC was partially supported by Fundación Andes. CMB acknowledges University of Chile graduate fellowship support from programs MECE Educación Superior UCH0118 and Fundación Andes C-13798.

References

Armandroff, T.E. & Da Costa, G.S., 1991, AJ 101, 1329
Bellazzini, M., Ferraro, F. R., and Ibata, R. 2003, AJ, 125, 188.
Bellazzini, M., Correnti, M., Ferraro, F. R., Monaco, L., and Montegriffo, P. 2006, A&A, L1.
Belokurov, V. et al. 2006, ApJ, 642, L137
Bonifacio, P. Sbordone, L., Marconi, G., Pasquini, L., and Hill, V. 2004, A&A 414, 503.
Bullock, J.S., Johnston, K.V., 2005, ApJ 635, 931
Buonanno, R., Corsi, C.E., Fusi Pecci, F., Fahlam, G.G., Richer, H.B., 1994, ApJ 430, L121
Buonanno, R., Corsi, C.E., Pulone, L., Fusi Pecci, F., Richer, H.B., Fahlam, G.G., 1995, AJ 109, 663
Carraro, G. 2005, ApJ, 621, L61
Carraro, G., Girardi, L., Chiosi, C., 1999, MNRAS 309, 430
Carrera, R., Gallart, C., Pancino, E., Zinn, R., 2007 AJ, submitted
Carretta, E., Gratton, R.G., 1997, A&AS 121, 95
Cenarro, A.J., Cardiel, N., Gorgas, J., Peletier, R.F., Vazdekis, A., Prada, F., 2001, MNRAS 326, 959
Cenarro, A.J., Gorgas, J., Cardiel, N., Vazdekis, A., Peletier, R.F., 2002, MNRAS 329, 863
Chou, Mei-Yin et al. 2006, ApJL, submitted (astro-ph/0605101)
Coelho, P., Barbuy, B., Meléndez, J., Schiavon, R.P., 2005, A&A in press (astro-ph/0505511)
Cohen, J. G. 2004, A.J., 127, 1545.
Cole, A.A., Smecker-Hane, T.A., Tolstoy, E., Bosler, T.L., Gallagher, J.S., 2004, MNRAS 347, 367
Coté, P., Diojrgovski, S.G., Meylan, G., McCarthy, J.K., 2002, ApJ 574, 783
Dinescu, D., Majewski, S.R., Girard, T. M, Cudworth, K. M., 2000, AJ 120, 1892
Duffau, S., Zinn, R., Vivas, A.K., Carraro, G., Méndez, R.A., Winninck, R., Gallart, C., 2006, ApJ 636, L97
Freeman, K., Bland-Hawthorn, J., 2002, ARA&A 40,487
Girardi, L., Bressan, A., Bertelli, G., Chiosi, C., 2000, A&AS, 114, 371
Grillmair, C. J., and Dionatos, 2006, ApJ, 643, L17
Grillmair, C. J. 2006, ApJ, 651, L29
Grillmair, C. J., Freeman, K.C., Irwin, M. & Quinn, P. J. 1995, AJ 109, 2553.
Harris, W.E. 1996, AJ, 112, 1487
Helmi, A., 2004a, MNRAS 351, 643
Helmi, A., 2004b, ApJ 610, L97
Horne, K., 1986, PASP, 98, 609
Johnston, K.V., Sigurdsson, S., Hernquist, L., 1999, MNRAS 302, 771
Kraft, R.P. & Ivans, I.I., 2003, PASP 115, 143
Koch, A., Grebel, E.K., Odenkirchen, M., Martínez-Delgado, D., Caldwell, J.A.R., 2004, AJ 128, 2274
Layden, A. C. & Sarajedini, A. 2000, AJ, 119, 1760
Law, D.R., Johnston, K.V., Majewski, S.R., 2005, ApJ 619, 803
Majewski, S.R., et al. 2003, ApJ 599, 1082
Majewski, S.R., et al. 2004, AJ 128, 245
Martinez-Delgado, D. et al. 2002, Ap.J., 573, L19
Martinez-Delgado, D., et al., 2004a, ApJ 601, 242
Martinez-Delgado, D. et al. 2004b, ASP conf. 327, 255
McWilliam, A. & Smecker-Hane, T. A. 2005, ASPS 336, 221
Monaco, L. et al. 2005, A&A 441, 141
Newberg, H. et al. 2002, ApJ 569, 245
Palma, C., Majewski, S. R., and Johnston, K. V. 2002, ApJ. 564, 736.
Pont, F., Zinn, R., Gallart, C., Hardy, E., Winnick, R., 2004 AJ 127, 840
Rosenberg, A., Saviane, I., Piotto, G., Aparicio, A., Zaggia, S.R.,1998a, AJ 115, 648
Rosenberg, A., Saviane, I., Piotto, G., Held, E.V., 1998b, A&A 339, 61
Salaris, M. & Weiss, A. 2002, A&A, 388, 492
Sandquist, E.L., 2004, MNRAS 347, 101
Sbordone, L., Bonifacio, P., Marconi, G., Buonanno, R., Zaggia, S., 2005, A&A 437, 905
Schlegel, D.J., Finkbeiner, D.P., Davis, M., 1998, ApJ 500, 525
Searle L, Zinn R., 1978, ApJ 225, 357
Stetson, P. B., 1994, PASP, 106, 250.
Stetson, P. B. et al. 1989, AJ, 97, 1360.
Tautvaisiene, G. et al. 2004, AJ, 127, 373
Tonry, J., Davis, M., 1979, AJ 84, 1511
Willman, B., Masjedi, M., Hogg, D.W., Dalcanton, J.J., Martinez-Delgado, D., Blanton, M., West, A.A., Dotter A., Chaboyer, B., 2006, ApJ in press (astro-ph/0603486)
Whiting, A.B., Hau, G.K.T., Irwin, M., 2002, ApJS 141, 123
Zinn, R. & West, M.J., 1984, ApJS 55, 45